1 **SUPPLEMENTARY MATERIAL (**all links accessible on 06/11/2024**)**

2 **Source data**

3   The BGC-Argo float dataset used in this study (WMO6903096) can be downloaded from the Argo Global
4 Data Assembly Center (https://data-argo.ifremer.fr/dac/coriolis/6903096/). These data were collected and made
5 freely available by the International Argo Program and the national programs that contribute to it:
6 (http://www.argo.ucsd.edu , https://www.ocean-ops.org). The Argo Program is part of the Global Ocean.
7 Observing System. UVP6 data can be downloaded from the EcoPart platform (project ID 36749;
8 http://ecopart.obs-vlfr.fr).

9

10 **Codes are available here:**
11 https://drive.google.com/drive/folders/1E0D_WfGT4PyeO5P7Idh9ZvXUlC9YkjdZ?usp=sharing

12 Packages used:
13 Umap function from umap-learn package in Phyton
14 Plotting_funcs for 2D grid interpolation and contours levels; Scipy for fitting curve and correlation;
15 mask_extreme; library("morphr"): ggmorph_tile; library(imager): clust_imgs; library("patchwork") wrap_plots;
16 library("vegan"): RDA ; library("chroma"); library("castr"); library("patchwork"); library("lubridate");
17 library("tidyverse"); library(dplyr); library("FactoMineR"); library("factoextra").

18
19 **Videos are available here**
20 Video of the trajectory of the float and sea level anomaly to track eddies:
21 https://drive.google.com/file/d/1sF4EhADEsXQ78XRY9q-nISAgNI44qhqz/view?usp=sharing
22 -Software used are: movavi maker , clideo.
23
24
25
26

27   **Morphological traits used for particle image classification**

Type	Parameter (variable name)	Description
Size	Area(area)	Number of pixel of the object
	Convex area (convarea)	Number of pixel of the smallest convex polygon that encloses the object
	Perimeter (perim)	Perimeter of the object
	Major axis length (major)	Length of the major axis of the ellipse fitted on the object
	Minor axis length (minor)	Length of the minor axis of the ellipse fitted on the object
Color	Median grey (mediangrey)	Median grey level values
	Coefficient of variation grey (cvgrey)	Ration of the standard deviation to the mean grey level values
	Integral grey (intgrey)	Sum of all grey level values
	Skewness grey (skewgrey)	Skewness of the histogram of grey level values
	Kurtosis grey (kurtgrey)	Kurtosis of the histogram of grey level values
Shape	Circularity (circ)	1 indicates a perfect circle, decreases as object moves away from a circle
	Elongation (elongation)	Major axis length to minor axis length ratio
	Extent (extent)	Ratio of pixels of the object to pixels in the total object bounding box
Complexity	Perim/Major (perimmajor)	Perimeter to major axis length ratio
	Solidity (solidity)	Ratio of object area to convex hull area
	Fractal dimension (fractal)	Fractal dimension of the object as defined in Maggi and Winterwerp (2004) and Many et al. (2019)

28   **Table S1: Morphological traits used for particle image classification**
29

30 **Sinking speed obtained by the lagged correlation over the full time series**

| Time lag (day)	3	6	9	12	15
All particles	0.25	0.56**	0.63**	0.42**	0.33**
MiP	0.23	0.34**	0.50**	0.39**	0.30**
MaP	0.26	0.50**	0.60**	0.38**	0.18
Flake	0.03	0.25	0.45**	0.28**	0.35**
Agglomerate	0.36**	0.63**	0.65**	0.37**	0.21
Strings	0.22	0.32**	0.36**	0.27	0.22
Spheres	0.23	0.44**	0.52**	0.35**	0.34**

31
32   **Table S2 : Lag Spearman correlations between the time series of particle abundance at 50-100m**
33 **and 300-400m. Significant correlation at 1% are indicated by **. The maximum correlation is always**
34 **observed at 9 days indicating an average sinking speed of 30.5 m d^{-1}.**
35

Sinking speeds and attenuation for different morphotypes

Cluster	Proportion in the population (%)	S(m d^{-1}) /A ESD: 0.65-0.81mm	S(m d^{-1}) /A ESD: 0.81-1.02 mm	S(m d^{-1}) /A ESD: : 1.02-1.29mm	S(m d^{-1}) /A ESD: 1.29-1.63mm	S(m d^{-1}) /A ESD: 1.63-2.05mm	S(m d^{-1}) /A ESD: 2.05-2.58mm
Flakes	26.83	15.86 (±2.68) /1.55(±0.14)	21.92 (±4.54) /1.59(±0.02)	16.29 (±4.43) /1.86(±0.21)	20.15 (±0.0) /1.82(±0.0)	NA	NA
Agglomerates	22.67	NA	NA	35.89 (±9.26) /0.88(±0.3)	31.04 (±19.70) /0.94(±0.23)	44.43 (±2.27)/ 0.70(±0.03)	56.67 (±7.72) /1.06(±0.04)
Strings	15.85	12.32 (±0.44) /1.47(±1.01)	12.03 (±7.68) /1.21(±0.42)	18.33 (±6.01) /1.76(±0.1)	NA	NA	NA
Spheres	34.64	26.31 (±1.05) /0.67(±0.02)	25.52 (±14.33) /0.50(±0.07)	46.09 (±24) /0.27(±0.23)	NA	NA	NA

37 **Table S3: Average and standard deviation of sinking speed (S) and attenuation rate (A) for four overlapping size ranges**
38 **among the morphotypes. The outliers values from the median have been removed and cases in which sinking speed**
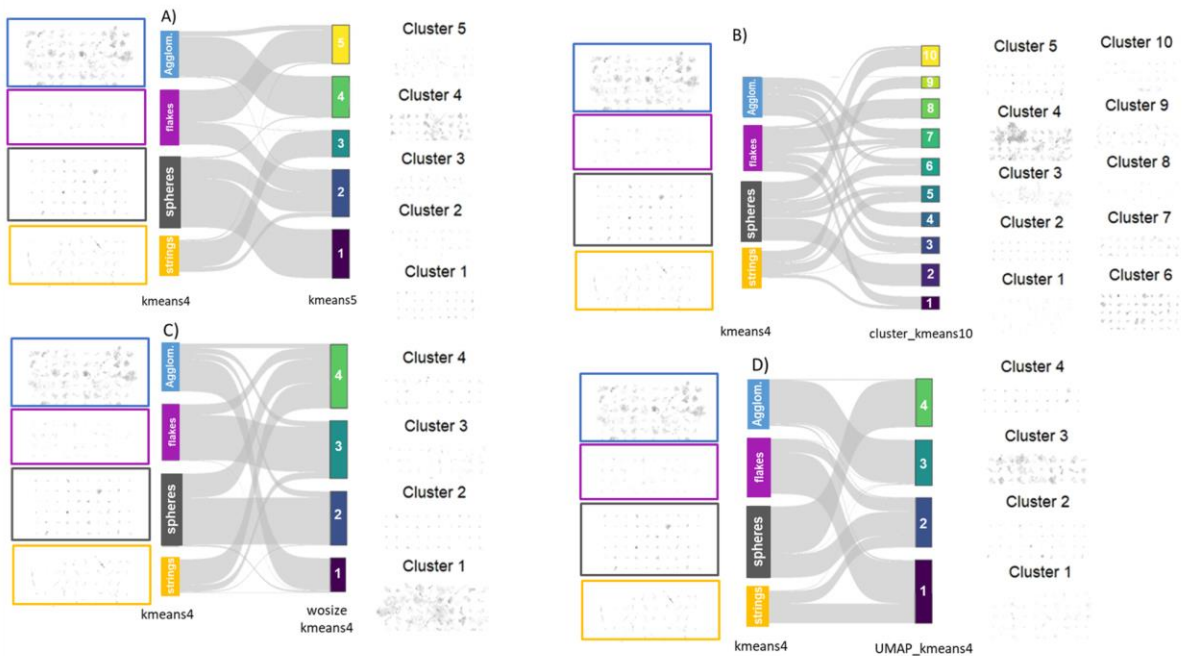39 **could not be determined are indicated by NA.**
40

PCA from traits used for particle and images after classification in four morphotypes
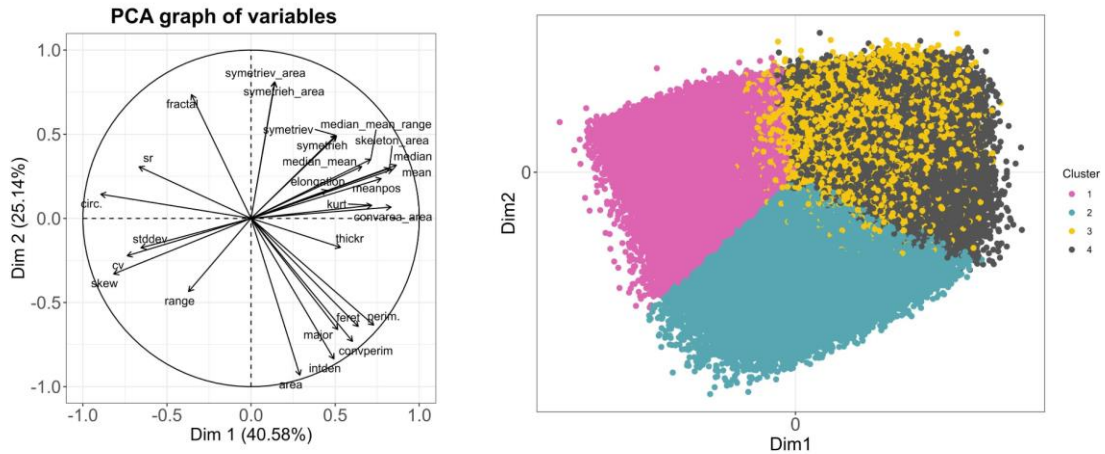
Figure S1: PCA from traits used for particle and images after classification in four morphotypes

**Sensitivity of aggregates classification to the method**

Figure S2 : Sensitivity of the quality of marine snow sorting to the number of categories from 4 to 5 in A) and from 4 to 10 in B); sensitivity to the use size as descriptor and in C) and comparing using U-map and PCA.

Marine snow particles encompass a broad diversity with continuous changes in morphology ranging from fresh fecal pellets produced by zooplankton with more defined shapes to porous and amorphous aggregates produced by coagulation via aggregates embedding fecal and other material (Trudnowska et al. 2021). Attempting to depict, automatically or manually, groups of similar aggregate types with identical ecological functions is deemed impossible (Trudnowska et al., 2021), or at best, only feasible for small datasets (Durkin et al. 2021). Likewise, defining the "true" number of aggregate categories in the water column is impossible due to the continuum of their morphology. Thus, the choice of categories has to be made operationally to be ecologically relevant, to remove possible classification bias, and to yield enough particles per category to allow the sinking speed estimates.

To assess whether our classification was representative of natural assemblages of marine snow and independent of size, we tested the effect of 1) the number of clusters, 2) sensitivity to size-related features, and 3) the method used to create the morphospace. We found that four clusters represented a satisfactory compromise providing meaningful categories. This may be attributed to limited availability of ecological data and the bias introduced by having more groups with fewer aggregates, thus resulting in less defined time series for calculating sinking speed. We opted for one fewer group than Trudnowska et al., (2021), as we had a more limited set of contextual information (notably no concomitant water collection to obtain ground truth biogeochemical data). Similarly to this previous work, the primary factor distinguishing the clusters was size, which had the greatest impact on structuring the morphospace. Removing all size-related features prior to the analysis surprisingly led to a similar morphospace suggesting that size is an important indirect variable in driving other aspects of morphology (i.e. smaller particles tend to have a higher probability of being dark and circular). Thus, comparing the clusterings revealed that aggregates of three out of four types tended to be grouped into similar associations. Defining a morphospace by using UMAP instead of PCA did not allow an interpretation of feature contribution. Nevertheless, we found a similar aggregates grouping, with three out of four clusters being dominated by the same type of aggregates as in the PCA variant.
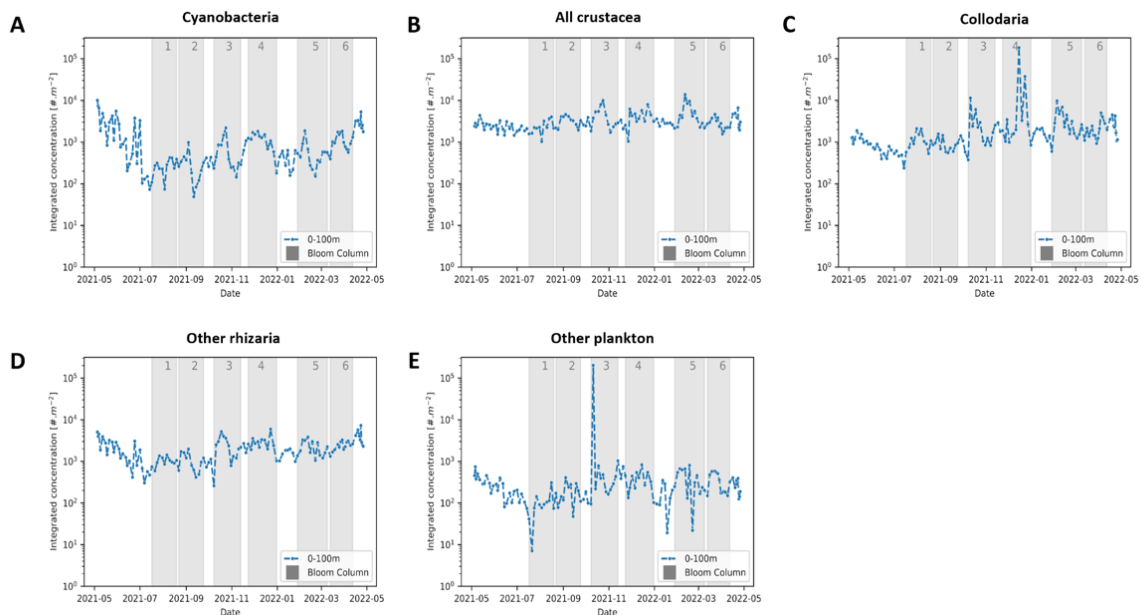
74   **ADT and surface Chl*a* at start and end of each periods**
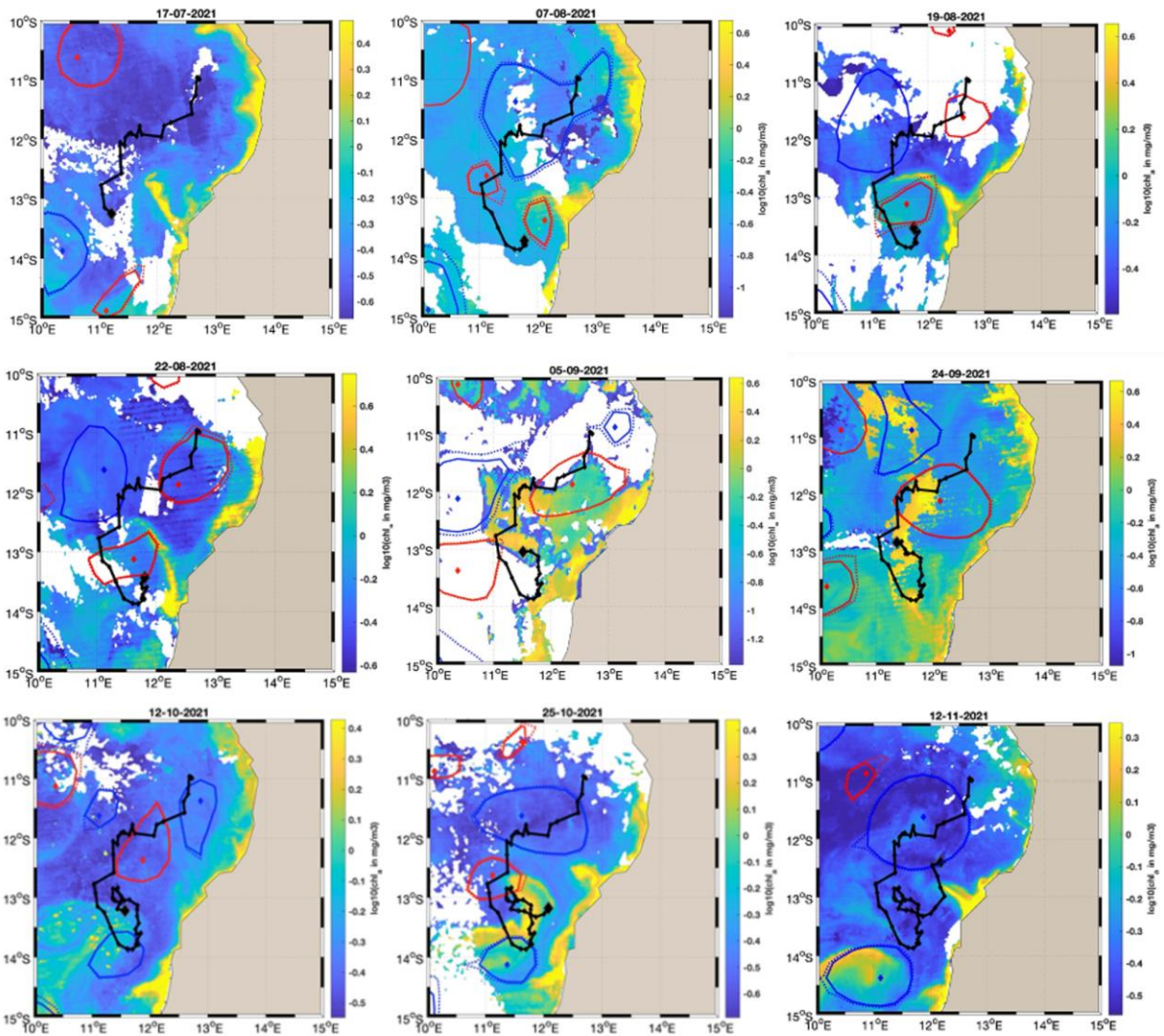
75
76   **Figure S3.1: ADT and surface Chla at first, second and third period (top panel to bottom panel) of the 3**
77   **first export events.**
78
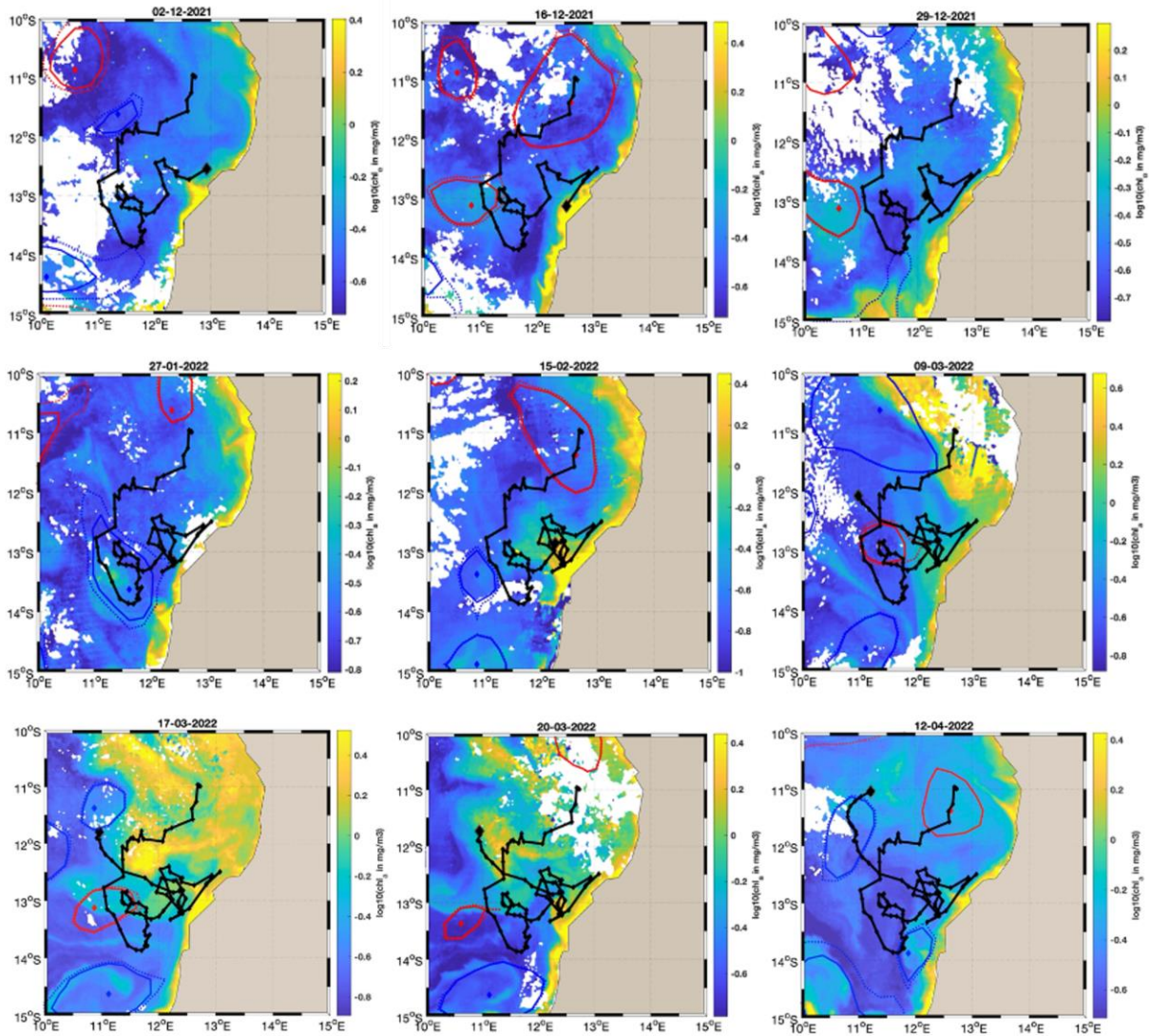
Figure S3.2: ADT and surface Chla at fourth, fifth period and end date (top panel to bottom panel) of the 3 last export events.
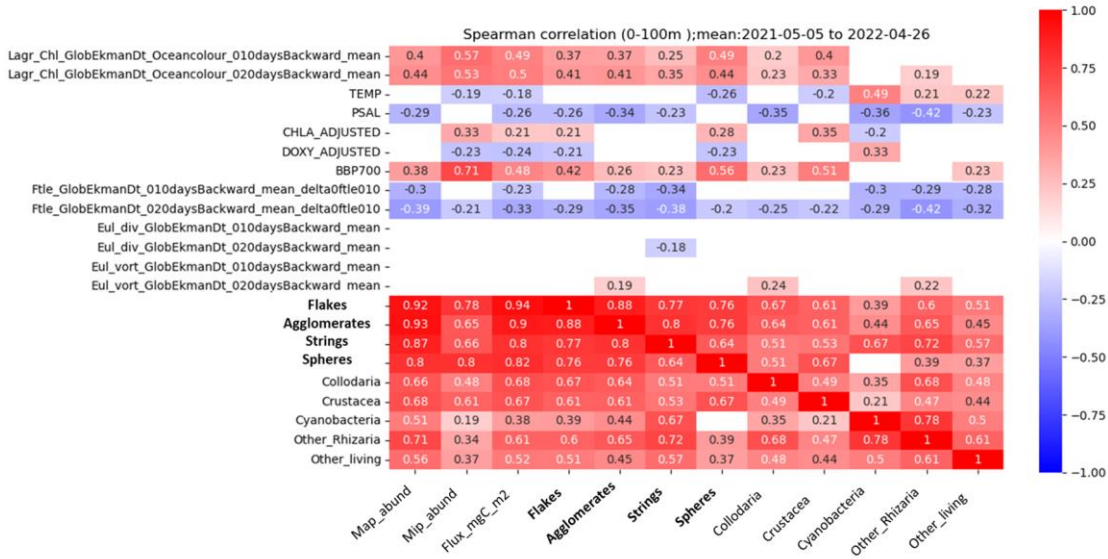
84 **Figure S4: Integrated concentrations (0-100m) of different categories of plankton as detected by**
85 **the UVP6 camera. A) Cyanobacteria/Trichodesmium (Puff+Tuff), B) all crustacea, C) Collodaria, D) other**
86 **rhizaria, and E) other plankton**

87

Spearman correlation (0-100m);mean:2021-05-05 to 2022-04-26

88
89 **Figure S5: Heat map of spearman correlations**

90 Comparing sensor's results from the BGC-Argo float, all types of marine snow and MiP are significantly
91 correlated to the Bbp while only flakes (cluster 1) and spheres (cluster 4) and MiP are correlated to the
92 fluorescence. Interestingly, flakes, agglomerates and strings (cluster 1, 2 and 3) are negatively correlated with
93 salinity. Correlations between Lagrangian Chl*a* and all marine snow types and plankton taxa are significant with
94 no lag for collodarians and crustaceans, a lag of 40 days for cyanobacteria, of 35 days for other taxa, 15 days for
95 phaeodaria. FTLE and all types of marine snow (but spheres (cluster 4)) and cyanobacteria, other taxa and other
96 Rhizarians are negatively correlated.

97

98
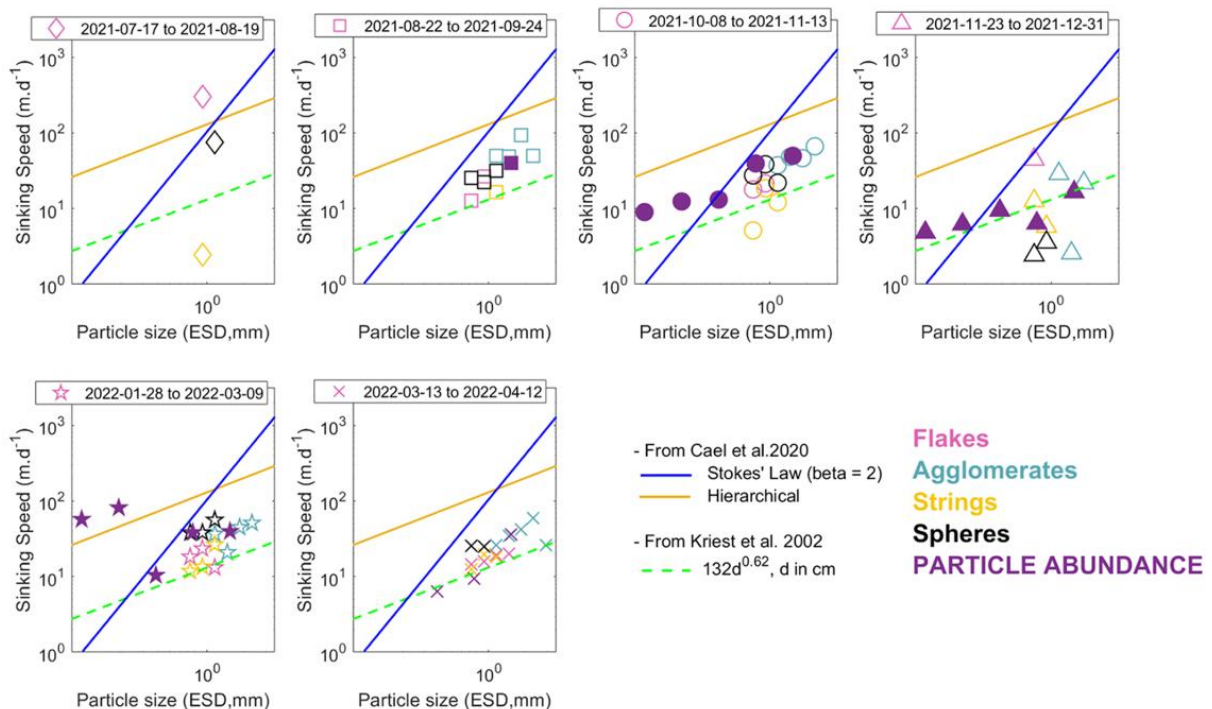
Figure S6 Sinking speed versus size during the 6 export events for the 4 different marine snow categories and the total particle abundance (MiP+MaP). The solid blue line is the Stokes' Law relationship, valid for spherical smooth particles with a constant excess density with increasing size and the orange line is the hierarchical regression on the data compilation in Cael et al., 2021. Dashed green line represents the model parametrizations of size-sinking relationship by Kriest et al., 2002.
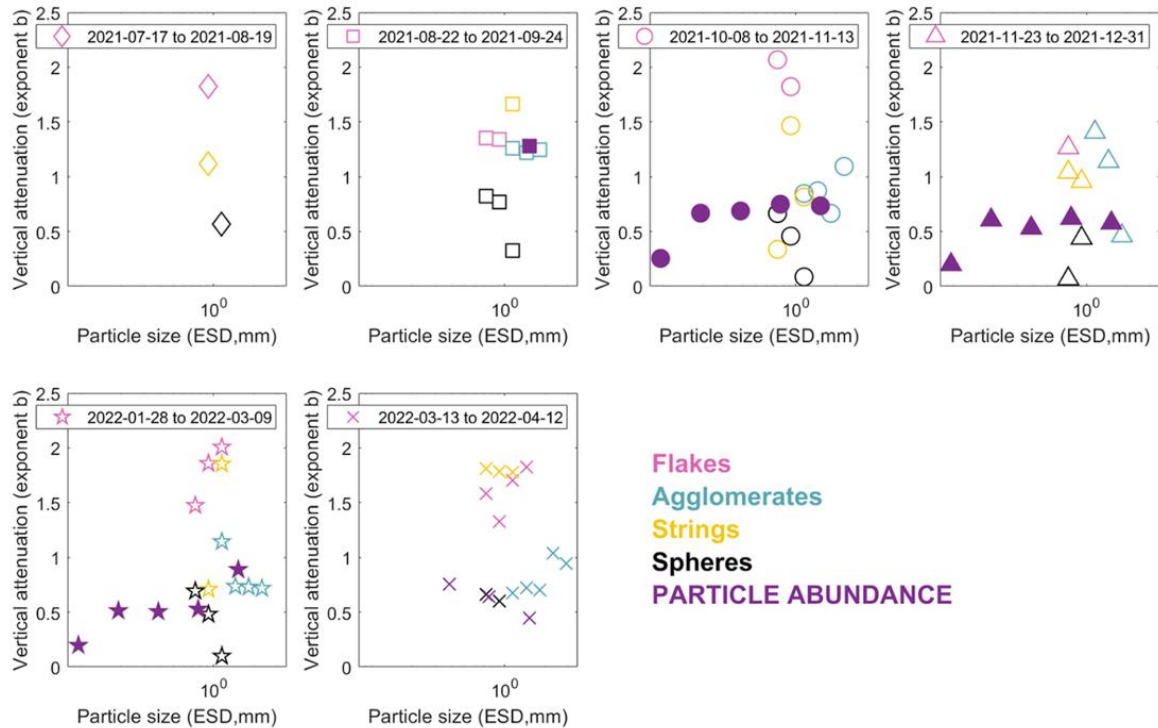
Figure S7: Attenuation exponent *b* versus size calculated during the six export events for the 4 different marine snow categories and the total particle abundance (MiP+MaP).